$$\left|-\frac{\pi}{2}\langle\Gamma_\lambda/\Gamma_{\lambda c(\lambda)}\rangle\langle(\Gamma_{\lambda c(\lambda)}/D)\Phi(\Gamma_\lambda/2D)\rangle \times[1-\langle\Gamma_\lambda/\Gamma_{\lambda c(\lambda)}\rangle\Gamma_{\mu c(\mu)}/\Gamma_\mu]\right|<1. \quad (A.8)$$

To remove the restrictions placed on the resonance structure at $E_\mu$, we must consider the following possible cases: (1) A second resonance $\nu$ has an $E_\nu$ unusually close to $E_\mu$. (2) A resonance lying close to $E_\mu$ has an unusually large width $\Gamma_{\lambda c(\lambda)}$. (3) $\mathfrak{U}_{cc}$ is evaluated at an off-resonance energy $E$. For cases 1 and 2 we must add to the factor $(\pi/2)\langle\Gamma_\lambda/\Gamma_{\lambda c(\lambda)}\rangle\langle\Gamma_{\lambda c(\lambda)}/D\Phi\rangle$ the expressions $\Gamma_{\nu c(\nu)}/\Gamma_\nu$ or $\Gamma_{\nu c(\nu)}/2D$, respectively. Case 3 is accounted for by setting $\Gamma_{\mu c(\mu)}/\Gamma_\mu=0$.

As in Sec. IV we now take $\Phi$ outside the averaging sign and we also replace $\Gamma_{\lambda c(\lambda)}/D$ by its maximum value $\Gamma_\lambda/D$. Then, supposing $\langle\Gamma_\lambda/\Gamma_{\lambda c(\lambda)}\rangle$ to be less than 2, the expression $|1-\langle\Gamma_\lambda/\Gamma_{\lambda c(\lambda)}\rangle\Gamma_{\mu c(\mu)}/\Gamma_\mu|$ will always be less than 1. We find then from (A.8) the convergence condition

$$2\pi(\langle\Gamma_\lambda\rangle/D)\Phi(\langle\Gamma_\lambda\rangle/2D)<\frac{4}{\langle\Gamma_\lambda/\Gamma_{\lambda c(\lambda)}\rangle}. \quad (A.9)$$

Consulting Fig. 3, one sees that this is satisfied if

$$\langle\Gamma_\lambda\rangle/D<\tfrac{1}{2} \quad \text{for} \quad \langle\Gamma_\lambda/\Gamma_{\lambda c(\lambda)}\rangle<2, \quad (A.10)$$

which is a reasonable limit on the effective channel number up to $\langle\Gamma_\lambda\rangle/D\sim1$. If the effective channel number is 1 then $\langle\Gamma_\lambda\rangle/D$ may approach unity. Also if $\langle\Gamma_\lambda\rangle/\langle\Gamma_{\lambda c(\lambda)}\rangle$ is appreciably larger than unity, the limit on $\langle\Gamma_\lambda\rangle/D$ is increased by a corresponding factor.

Of the three alternate conditions enumerated above, the third one does not affect our conclusions provided $\langle\Gamma_\lambda/\Gamma_{\lambda c(\lambda)}\rangle<2$, while the second one affects condition (A.10) only slightly. Because of the level repulsion effect, the first alternate condition may be expected to be applicable only when $\langle\Gamma_\lambda\rangle$ approaches $D$. It therefore gives a convergence limit of the same order of magnitude as (A.10). However as $\langle\Gamma_\lambda\rangle/D$ increases beyond unity, the overlapping resonances at any energy give rise to rapidly increasing numbers of terms making large contributions to expression (A.1), causing the series to diverge. In fact for $\langle\Gamma_\lambda\rangle\gg D$ the expression (A.1) approaches $(\langle\Gamma_\lambda\rangle/D)^n$ in order of magnitude.

In view of the several approximations made in deriving Eq. (A.5), it is reasonable to conclude that in general the series converges and the results of Sec. III are valid when the average total width is less than the average level spacing and the effective number of channels is less than about two.

A second method proposed by Thomas,[6] employing the channel elimination method, leads to an expansion of the $R$ matrix which may under certain conditions have a much larger range of validity than that indicated above. However, in performing the inversion of this $R$-matrix expansion which is still necessary to obtain an explicit scattering matrix, one is again left with an expansion whose convergence characteristics are very similar to those obtained here.

PHYSICAL REVIEW VOLUME 123, NUMBER 3 AUGUST 1, 1961

# Decay of $Tm^{172}$†

R. G. Helmer* and S. B. Burson
*Argonne National Laboratory, Argonne, Illinois*

(Received March 16, 1961)

The radioactive nuclide $_{69}Tm^{172}$ was produced by successive capture of two neutrons in erbium oxide enriched in $Er^{170}$. The irradiations were made in the Materials Testing Reactor at Arco, Idaho. In addition to three thulium activities, these samples contained six active contaminants. Pure thulium sources were obtained by use of an ion-exchange column. Studies were conducted with a 256-channel coincidence scintillation spectrometer. These measurements indicate the presence of at least 17 gamma-ray and 5 beta-ray transitions. The beta-ray spectrum was studied with a 180° magnetic beta-ray spectrometer. This spectrum was analyzed by use of a computer program compiled by the authors in collaboration with members of the Argonne Applied Mathematics Division. The level scheme proposed for $Yb^{172}$ has states with energies, spins, and parities of $0.0(0^+)$, $0.079(2^+)$, $0.260(4^+)$, 1.17(3), 1.46(2), 1.54(3), 1.60(1), 1.64(?), and 1.73(3) Mev. The total decay energy is found to be 1.88 Mev. The experimental data are consistent with the previously proposed interpretation that the first two excited states are members of a $K=0$ rotational band based on the ground state. The states at 1.46 and 1.54 Mev are interpreted as members of a rotational band with $K=2$. The states at 1.60 and 1.73 Mev are tentatively interpreted as members of a rotational band with $K=0$ and negative parity. It is suggested that the state at 1.17 Mev has $K=3$. From the analysis of the beta spectrum it is concluded that the ground state of thulium has $I=K=2$ and negative parity.

## INTRODUCTION

### Previous Studies

THE radioactive nuclide $_{69}Tm^{172}$, which decays to $Yb^{172}$ by $\beta^-$ emission, has been reported by Nethaway *et al.*[1] They obtained this isotope from the decay of $Er^{172}$ which was produced by two successive neutron captures in stable $Er^{170}$. The thulium activity was identified by its genetic relationship to the $Er^{172}$ activity. The mass assignment was verified by time-of-flight isotopic separation. The half-life of thulium was

† Work performed under the auspices of the U. S. Atomic Energy Commission.

* This material has been submitted in partial fulfillment of the requirements for the Ph.D. degree at the University of Michigan, Ann Arbor, Michigan.

[1] D. R. Nethaway, M. C. Michel, and W. E. Nervik, Phys. Rev. **103**, 147 (1956).

measured to be 63.6±0.3 hr. Gamma rays of 0.076, 0.18, 0.40, 1.09, 1.44, and 1.79 Mev were reported.

Excited states in $Yb^{172}$ are also populated by electron capture in $Lu^{172}$. The latter activity has been studied by several groups.[2–4] Wilson and Pool[2] have proposed a decay scheme with excited states at 0.079, 0.260, 0.530, 1.172, 1.283, 1.375, 1.662, (1.699), and 2.072 Mev. They have assigned spins, $K$ values, and parities to all of these states except the one at 1.699 Mev.

*Note added in proof.* The work of C. J. Orth and B. J. Dropesky, "Decay of $Er^{172}$ and $Tm^{172}$," Phys. Rev. **122**, 1295 (1961), which appeared after this report was accepted for publication, is in substantial agreement with our results.

## Source Production

The source material used throughout this investigation was $Er_2O_3$ enriched to 87% in $Er^{170}$. The irradiations were made primarily in the Materials Testing Reactor, Arco, Idaho, in a flux of approximately $2\times10^{14}$ neutrons $cm^{-2}$ $sec^{-1}$. A few irradiations were made in the Argonne CP-5 reactor in a flux of $3\times10^{13}$.

The activities of interest in this study are related as follows.

$$\begin{array}{ccccc} Er^{170} & \xrightarrow{(n,\gamma)} & Er^{171} & \xrightarrow{(n,\gamma)} & Er^{172} \\ & & \beta^-\downarrow 7.5\text{ hr} & & \beta^-\downarrow 50\text{ hr} \\ & & Tm^{171} & \xrightarrow{(n,\gamma)} & Tm^{172} \\ & & \beta^-\downarrow 2\text{ yr} & & \beta^-\downarrow 64\text{ hr} \\ & & Yb^{171} & & Yb^{172} \end{array} \qquad (1)$$

In addition to the above activities, observable amounts of $Tm^{170}$ (125 day), $Er^{169}$ (9 day), $Yb^{169}$ (35 day), $Yb^{175}$ (4 day), $Ho^{166}$ (1 day), and $Sc^{46}$ (85 day) were present. Because of these contaminants, in addition to the $Er^{171}$ and $Er^{172}$, chemical separations were made to produce pure thulium. For this purpose an ion-exchange column was used. The details of this procedure, as well as the methods of preparing the sources for the scintillation and beta-ray spectrometers are presented in Appendix I.

The 2-yr activity in $Tm^{171}$ is characterized by beta rays of 30 and 100 kev and a 0.067-Mev gamma ray. Their presence did not interfere with the measurements made in this study. The only remaining corrections were for the 0.965- and 0.88-Mev beta rays and 0.084-Mev gamma ray associated with the decay of $Tm^{170}$.

## Apparatus

In this investigation, three instruments were used: 180° magnetic internal-conversion-electron spectrographs, a 180° magnetic beta-ray spectrometer, and a 256-channel scintillation coincidence spectrometer. The scintillation spectrometer is used for both gamma-gamma and beta-gamma coincidence measurements. The gamma-ray detectors are $2\frac{1}{4}$-in. cubic NaI(Tl) crystals; an anthracene crystal $\frac{3}{16}$ in. thick by $1\frac{1}{2}$ in. in diameter is used as a beta-ray detector. For coincidence experiments, a single-channel pulse-height analyzer and "fast-slow" coincidence circuit ($2\tau=40$ nsec) are used to gate the multichannel analyzer.

# EXPERIMENTAL RESULTS

## Studies of Internal-Conversion Electrons

Internal-conversion-electron groups were observed that correspond to the $K$, $L_{II}$, $L_{III}$, $M$, and $N$ lines for a 0.0787-Mev transition and to the $K$ and $L$ lines for a 0.181-Mev transition. All of these lines have been reported[3] previously in the studies of $Lu^{172}$. In addition, a weak conversion line was observed which corresponds to the $K$-conversion group for a transition of about 0.145 Mev. As will be seen, the existence of this transition is verified by coincidence measurements.

Visual estimates of the relative intensities of the lines indicate that these results support the previous assignments of $E2$ character for both the 0.079- and 0.181-Mev transitions.[3]

## Scintillation Studies

### *Singles Spectrum*

The gamma-ray spectrum is shown in Fig. 1. The light lines show the energies and intensities of the individual components that are presumed to be present. It should be emphasized that this figure does not constitute an independent decomposition of the total singles spectrum. Rather, it represents more nearly a synthesis in which the relative intensities and approximate energies of many of the constituents are taken directly from the coincidence experiments. For example, the relative intensities of the 0.91-, 1.19-, 1.28-, 1.37-, and 1.47-Mev transitions are imposed from the values derived from the spectrum in coincidence with the 0.181-Mev transition. The heavy line, which is to be compared with the experimental points, represents the sum of the individual gamma rays shown. The spectral shapes of single gamma rays were interpolated from those of $V^{52}$ (1.42 Mev), $Na^{22}$ (1.28 and 0.511 Mev), $Zn^{65}$ (1.12 Mev), $Cs^{137}$ (0.662 Mev), and $Ce^{141}$ (0.142

[2] R. G. Wilson and M. L. Pool, Phys. Rev. **118**, 1067 (1960).
[3] J. W. Mihelich, B. Harmatz, and T. H. Handley, Phys. Rev. **108**, 989 (1957).
[4] Iu. G. Bobrov, K. La. Gromov, B. S. Dzhelepov, and B. K. Preobrazhenskii, Izvest. Akad. Nauk S.S.S.R., Ser. Fiz. **21**, 940 (1947) [translation: Bull. Acad. Sciences U.S.S.R. **21**, 942 (1957)]; V. M. Kellman, R. Ia. Metskhvarishvili, B. K. Preobrazhenskii, V. A. Romanov, and V. V. Tuckhevich, Zhur. Eksptl. i Teoret. Fiz. U.S.S.R. **35**, 1309 (1958) [translation: Soviet Phys.—JETP **35**, 914 (1959)]; L. T. Dillman, R. W. Henry, N. B. Gove, and R. A. Becker, Phys. Rev. **113**, 635 (1959).

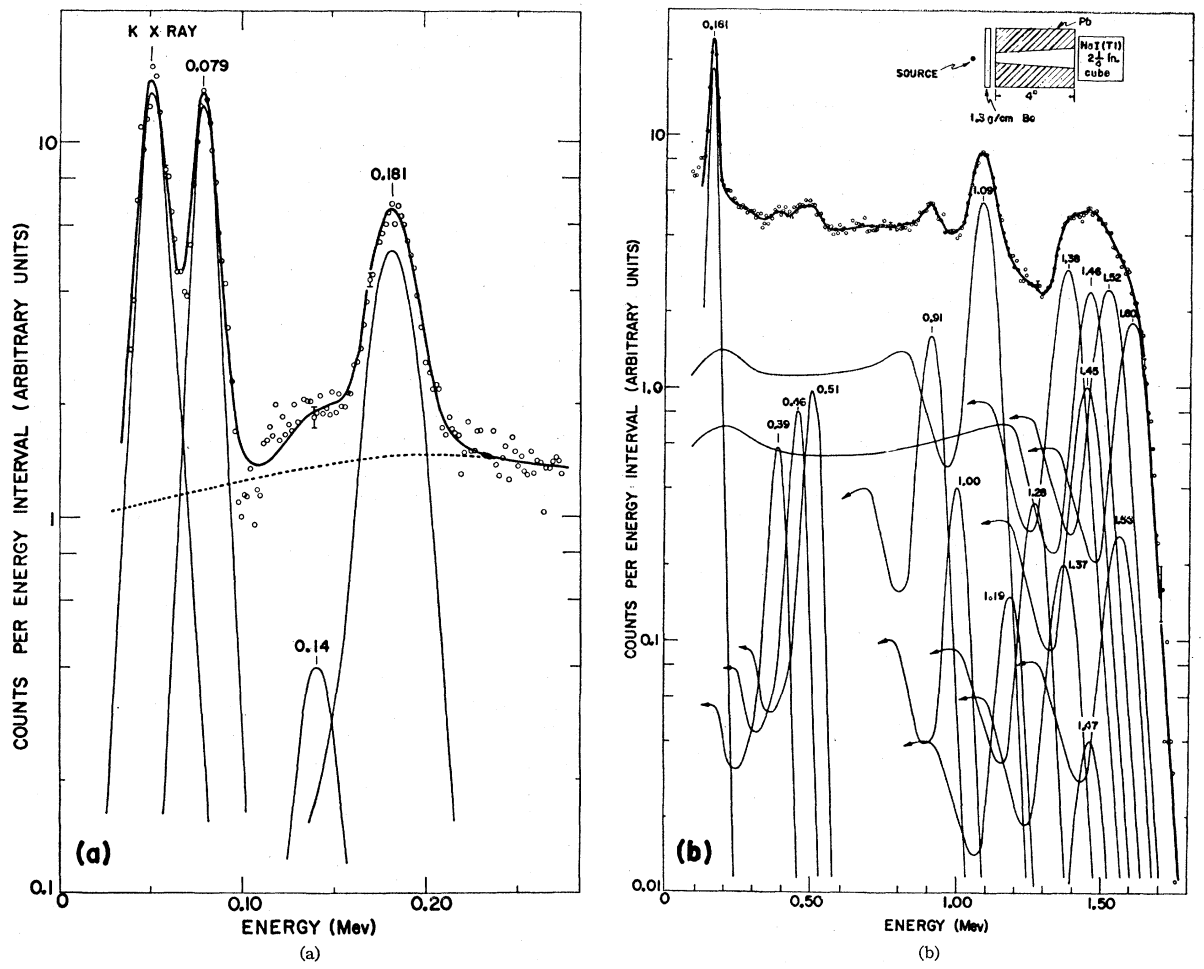


FIG. 1. Gamma-ray spectrum of $Tm^{172}$. The dashed line in (a) represents the sum of the gamma rays whose energies are above 0.2 Mev. The heavy line, which is to be compared with the experimental points, represents the sum of the individual gamma rays shown.

Mev). A summary of the relative photon intensities calculated from this spectrum is given in Table I.[5]

### *Gamma-Gamma Coincidence Experiments*

A large number of coincidence measurements were made in order to determine the energies and intensities of the radiations present, as well as to determine their positions in the decay scheme.

In order to ascertain the coincidence relationships between the radiations with energies above 1 Mev and those below 0.4 Mev, the region between 1.1 and 1.6 Mev was scanned with the single-channel analyzer. A window approximately 35 kev wide was used and 13 coincidence spectra were taken. Figure 2 is an example of this series. This spectrum, taken in coincidence with the pulses in the energy interval between 1.46 and 1.50 Mev, was selected because the photopeak at 0.14 Mev, which was not apparent in the singles spectrum, demonstrates the existence of a gamma ray of this

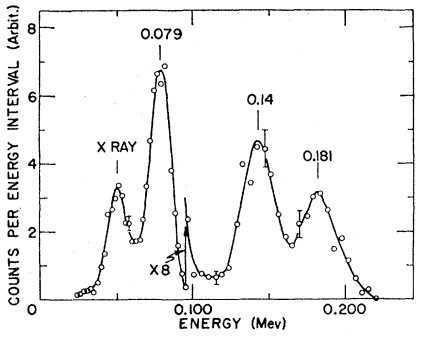


FIG. 2. Gamma-ray spectrum in coincidence with pulses in the range from 1.46 to 1.50 Mev.

[5] During a recent conversation, P. Gregers Hansen of the Chemistry Division, Atomic Energy Commission, Research Establishment Risø, Roskilde, Denmark showed the authors a gamma-ray spectrum measured with a three-crystal pair spectrometer. This spectrum exhibited four well-resolved gamma rays that the authors interpreted as those corresponding to the four strongest photopeaks in this decomposition above 1.2 Mev (i.e., the 1.38-, 1.46-, 1.52-, and 1.60-Mev transitions). This fact is noted in support of the foregoing analysis.

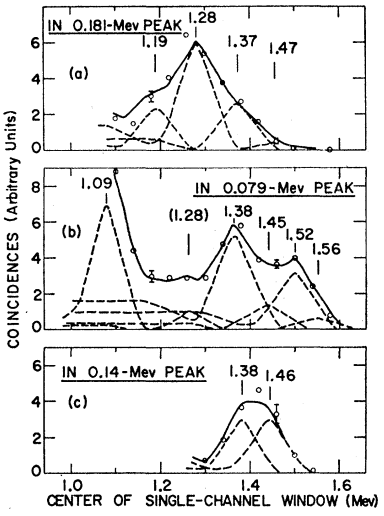


FIG. 3. Summary of coincidence spectra. The areas of the photopeaks at (a) 0.181, (b) 0.079, and (c) 0.14 Mev are plotted as a function of the energy corresponding to the center of the single-channel window.

energy. (The observation of $K$-conversion electrons for this transition has been noted above.) The analysis of the 13 coincidence spectra is presented in Fig. 3. The intensities of the three low-energy transitions (0.079, 0.14, and 0.181 Mev) are plotted as functions of the energy corresponding to the center of the single-channel window. The dashed lines indicate the energies and intensities of the individual radiations presumed to be present. The interpretation of these spectra is presented in the succeeding paragraphs.

The relationships suggested by the above data were further studied by setting the single-channel window on each of the three low-energy photopeaks. The results of these runs are presented in Fig. 4. As before, the

TABLE I. Gamma-ray energies and relative intensities calculated from the decomposition of the scintillation spectrum.

| Transition energy (Mev) | Relative photon intensities |
|---|---|
| 1.60 ±0.015 | 73 ±15 |
| 1.56 ±0.02 | 12 ±8 |
| 1.52 ±0.015 | 93 ±15 |
| 1.47 ±0.03 | 1.0±0.7 |
| 1.46 ±0.015 | 79 ±20 |
| 1.45 ±0.02 | 34 ±15 |
| 1.38 ±0.015 | 93 ±15 |
| 1.37 ±0.025 | 4.4± 1 |
| 1.28 ±0.02 | 8 ± 1 |
| 1.19 ±0.03 | 3.5±0.7 |
| 1.09 ±0.01 | 112 |
| 1.00 ±0.02 | 6 ± 5 |
| 0.91 ±0.01 | 24 ± 4 |
| 0.51 ±0.025 | 6 ± 2 |
| 0.46 ±0.025 | 4.4± 2 |
| 0.39 ±0.03 | 3 ± 1 |
| 0.181±0.004 | 35 ± 2 |
| 0.142±0.008 | 2.4± 1 |
| 0.079±0.002 | 47 ±12 |
| x ray | 63 ±16 |

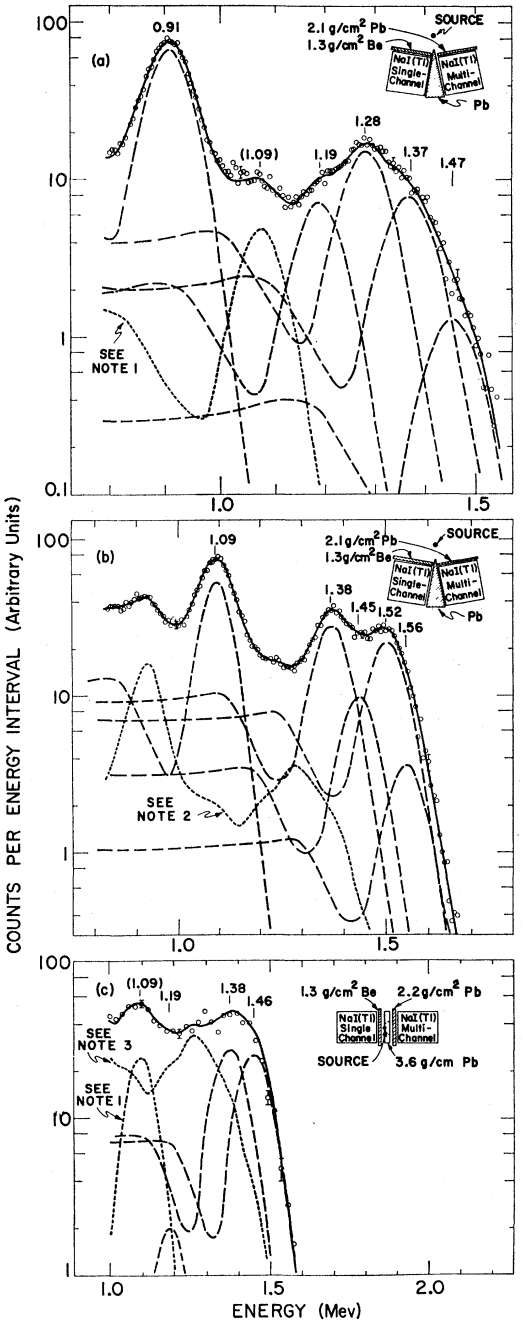


FIG. 4. Gamma-ray spectra in coincidence with (a) the 0.181 Mev, (b) the 0.079-Mev, and (c) the 0.14-Mev transitions. In curves (a) and (c), the 1.09-Mev photopeak is interpreted as being due to coincidences with back-scattered radiation from gamma rays whose energies are from 0.4 to 0.5 Mev. The dotted curve represents the radiations which are in coincidence with the 0.079-Mev transitions via the 0.181-Mev transition. This curve represents coincidences with the 0.181-Mev gamma ray.

decompositions into individual components are shown. In the spectrum of radiations in coincidence with the photopeak at 0.181 Mev, Fig. 4(a), the peak at 1.09 Mev is interpreted as being due to coincidences with

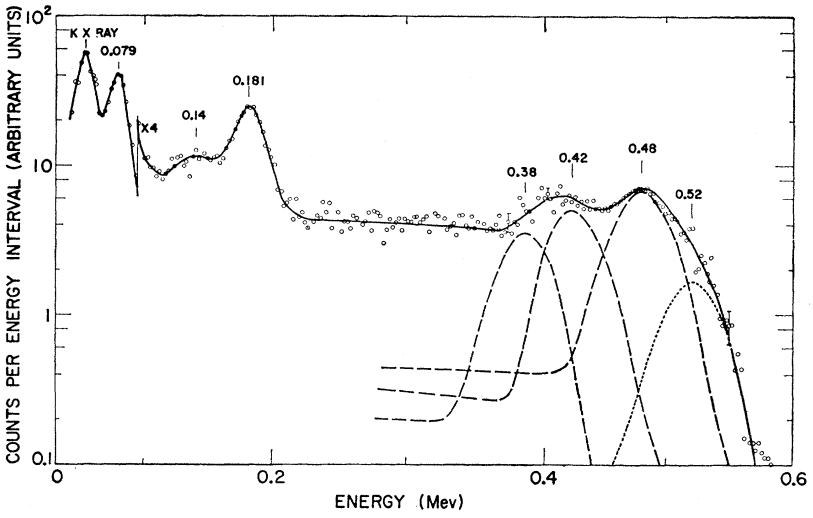


FIG. 5. Gamma-ray spectrum in coincidence with the 1.09-Mev transition.

backscattered radiation arising from gamma rays of 0.35–0.50 Mev. (It will be shown later that these coincidences exist.) This interpretation is supported by the absence of a corresponding peak at 1.09 Mev in Fig. 3(a). With the exception of the 1.09-Mev photopeak, the curves in Figs. 3(a) and 4(a) are practically identical. Therefore, it is concluded that the 0.181-Mev transition is in coincidence with gamma rays at 1.47, 1.37, 1.28, 1.19, and 0.91 Mev.

The gamma rays of 0.079 and 0.181 Mev are in cascade. (The experiments demonstrating this relationship are not described.) From their intensities as well as the studies[2] of $Lu^{172}$, it is apparent that the 0.079-Mev transition goes to the ground state, and the 0.181-Mev transition goes from the second excited state at 0.260 Mev to the 0.079-Mev level. Therefore, the spectrum in coincidence with the 0.079-Mev photopeak, Fig. 4(b), also shows the radiations found in coincidence with the 0.181-Mev transition [Fig. 4(a)]. The resulting analysis of Fig. 4(b) indicates that the 0.079-Mev level is fed directly by transitions of 1.56, 1.52, 1.45, 1.38, and 1.09 Mev. Again the data in Fig. 3(b) are consistent with this interpretation.

When the single-channel window is set to bracket the region of the weak 0.14-Mev radiation, most of the pulses registered arise from the spectral background. In Fig. 4(c) the dotted curves correspond to radiations that are interpreted as resulting from coincidences with this spectral background. The peaks at 1.46, 1.38, and 1.19 Mev are interpreted as representing gamma rays which are in coincidence with the 0.14-Mev transition. These conclusions are supported by the spectrum in Fig. 3(c).

One observes the spectrum shown in Fig. 5 when the single-channel analyzer is set to bracket the 1.09-Mev photopeak. This indicates the 1.09-Mev transition is in coincidence with gamma rays at about 0.52, 0.48, 0.42, and 0.38 Mev as well as 0.079 Mev. The peaks at 0.181 and 0.14 Mev are due to coincidences with higher energy transitions whose Compton distributions are counted in the single-channel window. The unresolved radiations below 0.35 Mev may be in coincidence with either the 1.09-Mev gamma ray or the underlying Compton distributions. When the single-channel window is moved to the 0.91-Mev photopeak, the observed spectrum is similar to this one, except for a strong 0.181-Mev peak. Therefore, it is concluded that the 0.91-Mev transition is also in coincidence with the gamma rays of 0.52, 0.48, 0.42, and 0.38 Mev as well as those of 0.181 and 0.079 Mev.

All of the coincidence data are summarized in Table II. Relative gamma-ray intensities calculated from these coincidence spectra are also given.

TABLE II. Gamma-gamma coincidences observed and relative gamma-ray intensities calculated from these data.

| Gamma ray in single-channel window (Mev) | Coincident gamma rays (Mev) | Relative photon intensities |
|---|---|---|
| 0.181 | 1.47 | 4 |
| | 1.37 | 18 |
| | 1.28 | 33 |
| | 1.19 | 14 |
| | 0.91 | 100.0 |
| 0.079 | 1.56 | 13 |
| | 1.52 | 81 |
| | 1.45 | 31 |
| | 1.38 | 83 |
| | 1.09 | 100.0 |
| 0.14 | 1.46 | 100.0 |
| | 1.38 | 100 |
| | 1.19 | 6 |
| 1.09 | ~0.51 | ... |
| | ~0.47 | ... |
| | ~0.42 | ... |
| | ~0.38 | ... |

### *Beta-Gamma Coincidence Studies*

The energies of the beta rays in coincidence with the dominant gamma rays were measured by absorption in aluminum. From these data, end-point energies were determined for the beta rays in coincidence with the gamma rays of 0.079, 0.181, 0.91, 1.09, 1.38, 1.46, 1.52, and 1.60 Mev. The analysis of the data in the energy interval from 1.3 to 1.6 Mev required a decomposition of the coincidence spectra into individual components. The results of these coincidence measurements are summarized in Table III.

From the relative gamma-ray transition intensities, together with the beta-gamma coincidence data, it follows that the beta-ray branches of (1.72±0.12) and (1.83±0.07) Mev, in coincidence with the 0.181- and 0.079-Mev gamma rays, are in fact two different transitions.

The proposed decay scheme requires the 0.079-Mev gamma ray to be in coincidence with beta-ray branches of about 0.71, 0.42, and 0.28 Mev in addition to the one listed at 1.83 Mev. These were not observed because of the presence of stronger coincidences between the 0.084-Mev gamma ray of $Tm^{170}$ and a 0.88-Mev beta-ray component.

### *Beta-Ray Spectrum*

The Fermi plot of the beta-ray spectrum of $Tm^{172}$ is shown in Fig. 6. In the original data, more than 15 000 counts were collected at each point below 1.3 Mev. This spectrum includes the long-lived $Tm^{170}$ which has beta-ray branches of about 0.96 and 0.88 Mev.

As noted in the previous section, it was concluded from the analysis of beta-gamma coincidence data, together with the proposed decay scheme (Fig. 7), that there are two beta-ray transitions, differing in energy by 0.1815 Mev; the end-point of the higher energy branch is about 1.80 Mev. These two transitions go to the 0.260- and 0.079-Mev levels. The ground-state beta branch, if present, would then have an energy of about 1.88 Mev. The data in Fig. 6 are not sufficient to allow differentiation of these three components (i.e., conventional analysis is not possible).

TABLE III. Summary of beta-gamma coincidence results.

| Gamma-ray energy (Mev) | Coincident beta-ray energies (Mev) |
|---|---|
| 1.60, 1.52 | 0.30±0.04 |
| 1.46, 1.38 | 0.43±0.03 |
| 1.09, 0.91 | 0.74±0.06 |
| 0.181 | 1.72±0.12, ~0.74, ~0.36 |
| 0.079 | 1.83±0.07 |

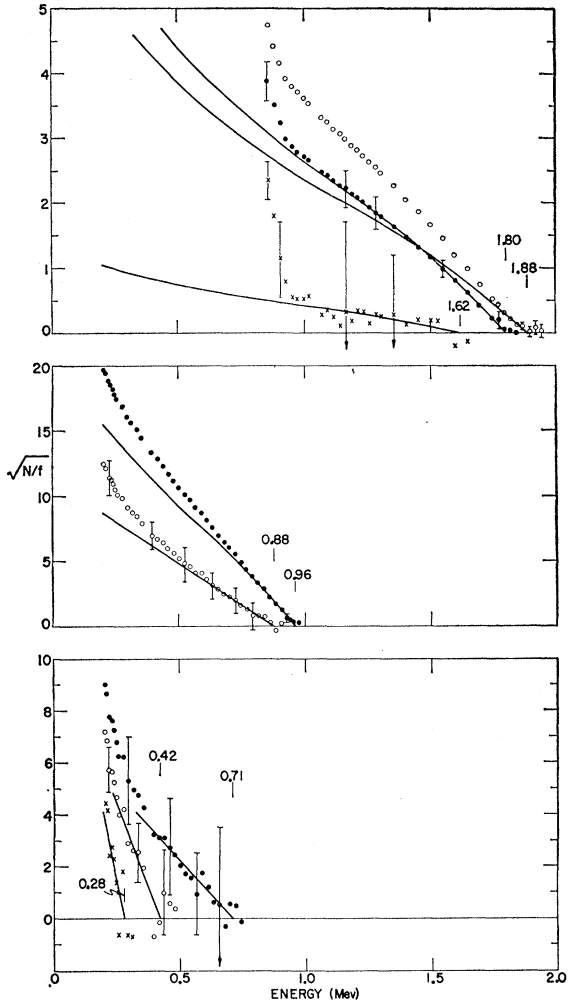


FIG. 6. Fermi plots of the beta-ray spectrum of $Tm^{172}$. The components shown in the middle diagram are associated with the decay of $Tm^{170}$.

This spectrum was analyzed by use of a computer program (discussed in Appendix II) that has been developed for the analysis of beta-ray spectra. Portions of the data were fitted with the function

$$\bar{N}=\sum_{j=1}^{J} m_j^2 f(\epsilon_{0j}-\epsilon)^2\{(1-\alpha_j) +\alpha_j[(\epsilon_{0j}-\epsilon)^2 L_0+9L_1]\}, \quad (2)$$

where the parameters to be varied are the $m_j^2$, $\epsilon_{0j}$, and $\alpha_j$. (Here $m_j$ is the slope of the linearized Fermi plot for the $j$th component, $\epsilon_0$ is the end-point energy, and $\alpha$ is related to the fraction of the component that is unique first forbidden.) The parameters are varied in order to minimize the function $\chi^2=\sum_i[(N_i-\bar{N}_i)/\sigma_i]^2$, where $N_i$ is the experimental counting rate, $\bar{N}_i$ is the counting rate calculated from (2), and $\sigma_i$ is the standard deviation associated with $N_i$.

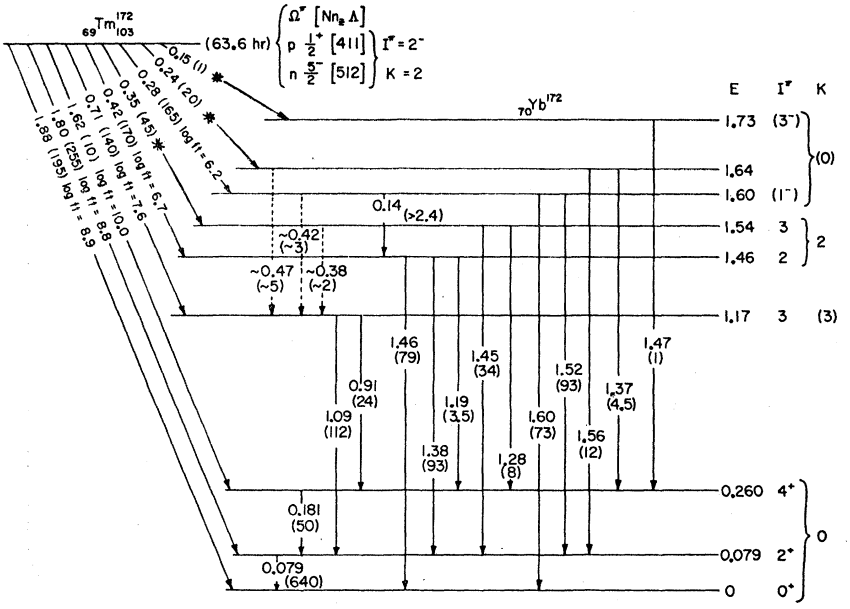


FIG. 7. Proposed decay scheme for $Tm^{172}$. The relative transition intensities (1000 total decays) are shown in parentheses. All energies are in Mev. The beta-ray branches denoted by an asterisk were not observed experimentally, but were inferred from the gamma-ray intensity data.

The data above 1 Mev were fitted on the assumptions of the presence of one, two, three, and four components ($J=1$, 2, 3, and 4). The end-point energies were related by $\epsilon_{01}-\epsilon_{02}=0.1815$ Mev for $J=2$, and $\epsilon_{01}-\epsilon_{02}=0.0787$ Mev and $\epsilon_{01}-\epsilon_{03}=0.2602$ Mev for $J=3$ and $J=4$, respectively. Thus, except for the case of $J=4$, there is only one independent energy parameter. The resulting values of $\epsilon_{0j}$, $\alpha_j$ and the relative intensities are given in fits Nos. 1–4 in Table IV. The value of $\chi^2$ is given in column 7. Column 8 gives the probabilities $p$ that any one set of experimental data from a large group of such sets would give a better fit to the assumed function.

In Table IV the uncertainties in the energies are those computed by the program, and include no systematic errors. The uncertainties in the relative intensities are calculated from the errors in the corresponding $m_j^2$ only, and neglect the effect of the errors in $\epsilon_{0j}$ and $\alpha_j$.

It is concluded from the data in Table IV that a beta transition to the ground state exists. This conclusion is based on the decrease in $p$ in going from the fit with two components to that with three. As shown, the addition of a fourth component in this region does not further decrease the value of $p$ and, in fact, the best fit is with zero intensity for a fourth component.

For the best fit, that with three components, the value $\alpha_2=0.63$ indicates that the second beta branch probably consists of a combination of an allowed shape and a unique-first-forbidden shape. The intensity of the allowed portion is $(6\pm6)\%$ of the total intensity. Therefore, this branch has predominantly unique-first-forbidden character. It should similarly be noted that the value $\alpha_1=\alpha_3=1.0$ means that these components have unique-first-forbidden character.

Below 1 Mev, the analysis of the $Tm^{172}$ spectrum is hampered by the presence of the $Tm^{170}$ spectrum consisting of two beta-ray components of about 0.96 and 0.88 Mev. The energy difference $\epsilon_{04}-\epsilon_{05}$, as determined from the reported gamma-ray energy, is 0.0842 Mev. The spectrum of $Tm^{170}$ has been studied by several groups.[6–8] Two of the more recent results[6,7] agree that the 0.88-Mev component constitutes about 24% of the total intensity and that its Fermi plot is linear. However, these reports[6,7] do not agree as to the shape of the Fermi plot of the 0.96-Mev transition. Pohm *et al.*[6] report that this component is linear ($\alpha_4=0$). The shape reported by Graham *et al.*[7] can not be expressed exactly in the form of Eq. (2); that is, it is not a linear combination of allowed and unique-first-forbidden shapes.

Because of this uncertainty in the shape of the Fermi plot of the 0.96-Mev transition, it is not possible to analyze the remainder of the spectrum unambiguously. Two attempts were made to fit the spectrum between 0.71 and 0.96 Mev. In the first case, the values of $\alpha_4$ and $\alpha_5$ were allowed to vary (e.g., see fit No. 5 in Table IV). The resulting parameters agree with the previous data[6,7] in that the 0.88-Mev component is linear ($\alpha_5=0$) and has an intensity of $(23\pm10)\%$. On the other hand, the shape of the 0.96-Mev branch is nonlinear ($\alpha_4=0.23$), which is not in agreement with the results of Pohm *et al.*,[6] but is in accord with the nonlinearity observed by Graham *et al.*[7] The second fit to the data

[6] A. V. Pohm, W. E. Lewis, J. H. Talboy, and E. N. Jensen, Phys. Rev. **95**, 1523 (1954).
[7] R. L. Graham, J. L. Wolfson, and R. E. Bell, Can. J. Phys. **30**, 459 (1952).
[8] See *Nuclear Data Sheets*, National Academy of Sciences, National Research Council (U. S. Government Printing Office, Washington, D. C.).

TABLE IV. Summary of computer fits to the beta-ray spectrum of $Tm^{172}$. The decomposition shown in Fig. 6 corresponds to results in fits Nos. 3, 5, and 6.

| Fit number | Energy range (Mev) | Number of components | Parameters from fit: Energy (Mev) | $\alpha$ | Intensity (arbitrary) | $\chi^2$ | $P$ |
|---|---|---|---|---|---|---|---|
| 1 | 1.00–1.87 | 1 | 1.847±0.003 | 0.30 | 4.6±0.7 | 60.9 | ≈0.99995 |
| 2 | 1.00–1.87 | 2 | 1.852±0.003 | 1.0 | 4.2 ±0.1 | 44.8 | 0.995 |
| | | | 1.671±0.003 | 1.0 | 0.7 ±0.1 | | |
| 3 | 1.00–1.87 | 3 | 1.880±0.011 | 1.0 | 2.1 ±0.7 | 22.6 | 0.57 |
| | | | 1.802±0.011 | 0.63 | 2.6 ±0.5 | | |
| | | | 1.620±0.011 | 1.0 | 0.07±0.2 | | |
| 4 | 1.00–1.87 | 4 | 1.880±0.011 | 1.0[a] | 2.1 ±0.7 | 22.6 | 0.57 |
| | | | 1.802±0.011 | 0.63[a] | 2.6 +0.5 | | |
| | | | 1.620±0.011 | 1.0[a] | 0.07±0.2 | | |
| | | | 0.0 | 0.0 | 0.0 | | |
| 5 | 0.38–0.98 | 6 | 1.880[a] | 1.0[a] | 2.1[a] | 16.3 | 0.36 |
| | | | 1.802[a] | 0.63[a] | 2.6[a] | | |
| | | | 1.620[a] | 1.0[a] | 0.07[a] | | |
| | | | 0.962±0.004 | 0.23 | 11.0 ±2.0 | | |
| | | | 0.878±0.004 | 0.0 | 3.2 ±1.0 | | |
| | | | 0.710[a] | 0.0[a] | 1.1 ±0.6 | | |
| 6 | 0.18–0.46 | 10 | 1.880[a] | 1.0[a] | 2.1[a] | 9.0 | 0.47 |
| | | | 1.802[a] | 0.63[a] | 2.6[a] | | |
| | | | 1.620[a] | 1.0[a] | 0.07[a] | | |
| | | | 0.962[a] | 0.23[a] | 11.0[a] | | |
| | | | 0.878[a] | 0.0[a] | 3.2[a] | | |
| | | | 0.710[a] | 0.0[a] | 1.1[a] | | |
| | | | 0.420[a] | 0.0[a] | 1.3 ±0.6 | | |
| | | | 0.340[a] | 0.0[a] | 0.0 | | |
| | | | 0.280[a] | 0.0[a] | 1.2 ±1.0 | | |
| | | | 0.240[a] | 0.0[a] | 1.9 ±2.0[b] | | |
| 7 | 0.46–0.98 | 6 | 1.880[a] | 1.0[a] | 2.1[a] | 15.6 | 0.26 |
| | | | 1.802[a] | 0.63[a] | 2.6[a] | | |
| | | | 1.620[a] | 1.0[a] | 0.07[a] | | |
| | | | 0.963±0.004 | 0.0[a] | 13.8 ±1.2 | | |
| | | | 0.878±0.004 | 0.0[a] | 0.3 ±1.2 | | |
| | | | 0.710[a] | 0.0[a] | 0.44±0.4 | | |
| 8 | 0.18–0.46 | 8 | 1.880[a] | 1.0[a] | 2.1[a] | 10.1 | 0.48 |
| | | | 1.802[a] | 0.63[a] | 2.6[a] | | |
| | | | 1.620[a] | 1.0[a] | 0.07[a] | | |
| | | | 0.963[a] | 0.0[a] | 13.8[a] | | |
| | | | 0.878[a] | 0.0[a] | 0.3[a] | | |
| | | | 0.710[a] | 0.0[a] | 0.66±0.4 | | |
| | | | 0.420[a] | 0.0[a] | 1.8 ±0.4 | | |
| | | | 0.280[a] | 0.0[a] | 2.0 ±1.0[b] | | |

[a] These parameters were not allowed to vary.
[b] These intensities are expected to be too large because of the presence of electron scattering in the source at low energies.

in this region (see No. 7, Table IV) was made on the assumption that both components are linear ($\alpha_4=\alpha_5=0$). The quality of the fits, as given by the values of $p$, gives no basis for a choice between these two cases, except that in the former case the relative intensities are in better agreement with the experimental results. However, this is not sufficient to discard the second fit, for the following reason. The total Fermi plot published by Graham *et al.*[7] appears to be almost linear. Thus, a combination of two linear components might very well result in a good over-all fit to the experimental data but still contain a large error in the relative intensities. Therefore, the analysis of the spectrum below 0.71 Mev was carried out for both of these cases.

The beta-ray intensities, as derived from the gamma-ray intensities, suggest that all the components below 0.8 Mev (see Fig. 7) have allowed or ordinary-first-forbidden character. Therefore, the corresponding $\alpha_j$ were all set equal to zero. Also, the end-point energies of all the branches were fixed at those values determined from the gamma-ray energies together with the proposed decay scheme. The resulting relative intensities are given in fits Nos. 5, 6, 7, and 8 in Table IV. The two sets of relative intensities for the components below 0.8 Mev, corresponding to $\alpha_4=0$ and $\alpha_4=0.23$, agree within one standard deviation. However, the intensity of the 0.71-Mev component calculated with $\alpha_4=0.23$ is in much closer agreement with the value calculated from the gamma-ray intensities. Therefore, the values from this decomposition (Nos. 3, 5, and 6) are shown in Table V and Fig. 6.

The end-point energies, relative intensities, and $\log ft$ values are shown in Table V. It should be noted that the relative intensities from the analysis of the beta-ray

TABLE V. Summary of beta-ray components.

| Energy (Mev) | Relative intensity: From gamma intensities (percent) | Relative intensity: From beta spectrum (percent) | Log$ft$ |
|---|---|---|---|
| 1.88±0.02 | (20) | 24± 8 | 8.9 |
| 1.80 | 25 | 29± 6 | 8.0 |
| 1.61 | 1± 1 | 1± 3 | 10.0 |
| 0.71 | 14± 2 | 12± 6 | 7.6 |
| 0.42 | ≤17 | 15± 7 | 6.7 |
| 0.34 | 4± 3 | ... | 7.0 |
| 0.28 | ≥17 | 13±10 | 6.2 |
| 0.24 | 2 ± 1 | ... | 6.8 |
| 0.15 | 0.1±0.3 | ... | 7.6 |

spectrum are in excellent agreement with those computed from the gamma-ray intensities.

The statistical evaluation of the fit to the complete spectrum is compatible with the data. For 68 experimental points, the value $\chi^2$ is 47.9. For 17 variable parameters this corresponds to $p=0.36$; that is, the probability of obtaining a better fit is only 36%

The log$ft$ values of the three highest energy transitions indicate that they all have unique-first-forbidden character ($\Delta I=2$, yes). This conclusion is supported by the spectral shape, at least for the two higher energy components. The log$ft$ values of the lower energy transitions all lie in the range from 6 to 8, which normally corresponds to ordinary-first-forbidden transitions ($\Delta I=0$ or 1, yes).

## DECAY SCHEME

### Construction of Level Scheme

The proposed decay scheme is shown in Fig. 7. The existence of levels at 0.079 and 0.260 Mev is in agreement with a diverse group of experimental data Coulomb excitation experiments[9] suggest the presence of an excited state at 0.079 Mev in $Yb^{172}$. As previously noted, the internal-conversion-electron data indicate that the 0.079-Mev gamma ray has $E2$ character. Using this fact together with the relative gamma-ray intensity in the thulium activity, one finds that this transition is more intense than the sum of all the other transitions. Hence, it must go directly to the ground state. Also the beta-gamma coincidence measurements reported herein require that both the 0.079- and 0.181-Mev gamma transitions must go to levels near the ground state. Finally, these two levels in $Yb^{172}$ are also populated in the decay of $Lu^{172}$. The gamma-gamma coincidences to be expected from the 0.079–0.181 Mev cascade were observed. (These spectra are not shown.)

The levels at 1.73, 1.64, 1.54, 1.46, and 1.17 Mev are indicated by the spectrum in coincidence with the 0.181-Mev gamma ray. It is seen that this gamma ray is in coincidence with gamma rays of 1.47, 1.37, 1.28, 1.19, and 0.91 Mev. The absence of coincidences between any two of the latter transitions and the fact that the sum of any pair exceeds the total decay energy of about 1.9 Mev both support this interpretation.

Of the five radiations in coincidence with the 0.079-Mev gamma ray and not in coincidence with the 0.181-Mev gamma ray [Fig. 4(b)], four (1.56, 1.45, 1.38, and 1.09 Mev) are associated with transitions to the first excited state from levels deduced in the previous paragraph. The 1.46-Mev gamma ray observed in the singles spectrum (Fig. 1) is interpreted as the transition from the level at 1.46 Mev to the ground state. The fifth radiation, 1.52 Mev, is placed between a level at 1.60 Mev and the first excited state. The existence of this level is further supported by observation of the 1.60-Mev crossover transition in the singles spectrum.

The experiments involving the 0.14-Mev gamma ray support a number of features of the decay scheme. This transition is placed between the levels at 1.46 and 1.60 Mev. Observation of coincidences between the 0.14-Mev gamma ray and radiations of 1.46, 1.38, and 1.19 Mev tends to confirm this conclusion.

The radiations of approximately 0.47, 0.42, and 0.38 Mev, which are in coincidence with the 1.09-Mev gamma ray (Fig. 5), are interpreted as transitions to the 1.17-Mev level from the states at 1.64, 1.60, and 1.54 Mev.

There are a few weak transitions which have not been discussed. In the analysis of the singles spectrum, there are gamma rays of about 1.00 and 0.51 Mev. There is also evidence that a transition of about 0.52 Mev and several possible radiations below 0.35 Mev are in coincidence with the 1.09-Mev gamma ray. Since there is no evidence to clearly indicate the positions of these radiations in the decay scheme, they are omitted from it.

The results of the beta-gamma coincidence measurements (Table III) substantiate the existence of the proposed levels at 1.17, 1.46, and 1.60 Mev as well as the placement of the transitions depopulating these levels.

Estimates of the relative intensities of the gamma-ray and beta-ray transitions (total number of transitions =1000) are given in parentheses. For the transitions above 0.4 Mev, internal conversion is assumed to be negligible. As noted, conversion-electron measurements[3] indicate that the 0.079- and 0.181-Mev transitions have $E2$ character. Hence the corresponding conversion coefficients were used in calculating these intensities. For the 0.14-Mev transition, the available conversion data are not sufficient to determine the multipolarity. Therefore, only a lower limit is quoted for the intensity.

### Spins and Interpretation of Levels

*Ground-State Rotational Band in $Yb^{172}$*

Since $Yb^{172}$ is an even-even nucleus, the spin and parity of its ground state are assumed to be $0^+$. Both

[9] E. L. Chupp, J. W. M. Dumond, F. J. Gordon, R. C. Jopson, and H. Mark, as reported by D. Strominger, J. M. Hollander, and G. T. Seaborg, Revs. Modern Phys. **30**, 585 (1958).

the Coulomb excitation data[9] and the fact that the 0.079-Mev transition is $E2$ require that the first excited state at 0.079 Mev have $2^+$ character. The $E2$ character of the 0.181-Mev transition requires that the spin of the state at 0.260 Mev should lie between 0 and 4 and that it should have positive parity. The ratio of energies of the levels agrees quite well with that predicted by the $I(I+1)$ interval rule for rotational levels with $I=2$ and 4. This fact, together with the systematics of even-even nuclei, suggests that these three levels form a rotational band with $K=0$, positive parity, and $I=0$, 2, and 4.

### *Thulium Ground State*

The ground-state spin of the odd-odd nucleus $_{69}Tm^{172}$ is expected to result from the coupling of the 69th proton and the 103rd neutron. The spin of the odd-$A$ nucleus $_{69}Tm^{169}$ has been measured[10] as $\frac{1}{2}$; Mottelson and Nilsson[11] have interpreted this as the Nilsson level $\frac{1}{2}^+[411]$. The spin[12] of $Er^{171}$ and that[13] of $Yb^{173}$, which have 103 neutrons, have both been measured as $\frac{5}{2}$; these have been interpreted[11] as the $\frac{5}{2}^-[512]$ level. In general, the resulting spin of $Tm^{172}$ would be given by $I=K=\Omega=|\Omega_p\pm\Omega_n|$, where $p$ and $n$ refer to the odd proton and neutron, respectively. If one assumes that the odd particles in $Tm^{172}$ are in the same states as in the neighboring odd-$A$ nuclei, this relationship gives $I^\pi=2^-$ or $3^-$. Gallagher and Moszkowski[14] have derived coupling rules which predict that the ground state will be the one in which the projections of the intrinsic spins lie in the same direction. For $Tm^{172}$, this rule predicts that the $I^\pi=2^-$ state should be the ground state. However, several exceptions to these coupling rules are known.

The spin of the ground state of thulium is determined from the properties of the beta decay to the $K=0$ rotational band. The choice $I=K=3$ can be excluded, since the decay to the ground state of ytterbium would be third forbidden ($\Delta I=3$, yes) and should have a log$ft$ value of approximately 15. If $K$ is a good quantum number, the transitions to the first and second excited states would likewise be third forbidden because of the change in the quantum number $K$ ($\Delta K=3$). However, the measured log$ft$ values are about 9 for all three branches. On the other hand, for the choice $I=K=2$ the calculated log$ft$ values agree with those observed experimentally. The unique-first-forbidden shape for the transition to the $2^+$ level is explained by the change of the quantum number $K$. It should be pointed out that the assignment $I=K=2$ could be deduced without recourse to the arguments concerning the Nilsson levels and the spins of the individual particles.

This assignment is further supported by the agreement between the experimental and theoretical ratios between the beta-ray branches to the members of the ground-state rotational band. For the case of $L=2$ transitions, the theoretical ratios are

$$B(2,\ 2\rightarrow 4):B(2,\ 2\rightarrow 2):B(2,\ 2\rightarrow 0)=0.5:10:7,$$

where $B(2,\ 2\rightarrow I)=(\text{constant})|\langle 222-2|22I0\rangle|^2$. The corresponding experimental ratios $(0.35\pm0.30):10:(6\pm4)$, where $B=(\text{constant})/ft$, agree well within the experimental errors.

A restriction can now be placed on the choice of spins which may be assigned to levels in $Yb^{172}$. The beta-ray branches which populate these states are all ordinary-first-forbidden (or "slow" allowed) transitions, so that the spins of these levels must be 1, 2, or 3. Also, if one assumes that $K$ is a good quantum number, the value of $K$ for any of these states would similarly be limited to the values 1, 2, or 3.

TABLE VI. Theoretical relative reduced transition probabilities to the $I=4$, 2, and 0 members of a rotational band with $K=0$ from states with various values of $I$ and $K$. The ratios are given in the form $B(L, I\rightarrow 4):B(L, I\rightarrow 2):B(L, I\rightarrow 0)$, where $B(L, I_i\rightarrow I_f)=\text{constant}\times|\langle I_iLK_iK_f-K_i|I_iLI_fK_f\rangle|^2$. Where the values are not shown for $L=1$ or $L=2$, the three corresponding probabilities all vanish.

| | $K=3$ $L=3$ | $K=2$ $L=2$ | $K=1$ $L=2$ | $K=1$ $L=1$ | $K=0$ $L=2$ |
|---|---|---|---|---|---|
| $I=4$ | 10:11:0 | 3:1:0 | 9:110:0 | 1:0:0 | 10:11:0 |
| $I=3$ | 54:275:132 | 2:5:0 | 5:2:0 | 3:4:0 | 4:3:0 |
| $I=2$ | ··· | 1:20:14 | 96:15:56 | 0:1:0 | 18:10:7 |
| $I=1$ | ··· | ··· | 0:1:0 | 0:1:2 | 0:2:1 |
| $I=0$ | ··· | ··· | ··· | ··· | 0:1:0 |

### *State in Yb at 1.17 Mev*

The state at 1.17 Mev is depopulated by transitions to the $2^+$ and $4^+$ levels. The intensity of the transition to the $0^+$ state is less than 3% of that of the 1.09-Mev gamma ray. If only the changes in $I$ are considered, a spin of either 3 or 4 for the 1.17-Mev level would be consistent with these observations.

From the analysis of the experimental data, it is concluded that this state has $I=K=3$. This choice is made on the basis of the relative reduced transition probabilities to the various members of the ground-state band. The theoretical probabilities, which are listed in Table VI, are considered to be proportional to the squares of the Clebsch-Gordan coefficients $\langle I_iLK_iK_f-K_i|I_iLI_fK_f\rangle$. Without calculation of the magnetic and electric moments, the relative intensities for the two cases $I=4$, $K=1$ and $I=K=1$ are partially indeterminate. Hence, these possibilities are not considered in detail in the following discussion.

[10] K. H. Lindenberger, Z. Physik **141**, 476 (1955); H. Schüler and T. Schmidt, Naturwissenschaften **22**, 838 (1934).
[11] B. R. Mottelson and S. G. Nilsson, Kgl. Dankse Videnskab. Selskab, Mat.-fys. Skrifter **1**, No. 8 (1959).
[12] A. Y. Cabezas, I. P. K. Lindgren, and R. Marrus, Bull. Am. Phys. Soc. **5**, 343 (1960).
[13] A. H. Cooke and J. G. Park, Proc. Phys. Soc. (London) **A69**, 282 (1956); H. Schüler, J. Roig, and H. Korsching, Z. Physik **111**, 165 (1938).
[14] C. J. Gallagher, Jr., and S. A. Moszkowski, Phys. Rev. **111**, 1282 (1958).

For the 1.17-Mev state, the corresponding experimental values are

$$B(L, I\to 4):B(L, I\to 2):B(L, I\to 0)$$
$$=(1.8\pm0.4):5:(<0.1) \quad \text{for} \quad L=1,$$
$$=(2.6\pm0.6):5:(<0.1) \quad \text{for} \quad L=2,$$
$$=(3.8\pm0.8):5:(<0.1) \quad \text{for} \quad L=3.$$

The only theoretical prediction (see Table VI) that is within the experimental limits is the one for $I=3$, $K=2$. The transitions then have quadrupole character. However, this assignment for the $K$ value would imply that this state would be the first excited state of a rotational band based on an intrinsic or vibrational level with $I=K=2$. This hypothetical $I=2$ state, which should lie about 0.08 Mev below the 1.17-Mev level, is not observed, in spite of the fact that theoretically the beta branch to it would be more intense than that to the 1.17-Mev level.

It is therefore suggested that the 1.17-Mev state has $I=K=3$. This means that quadrupole transitions to the $K=0$ band are $K$ forbidden by one degree of forbiddenness (i.e., $\Delta K-L=1$). Such transitions usually are slower than the single-particle estimates by a factor of the order of 100. If the 1.17-Mev state has positive parity, the competition is between $E2$ and $M3$ transitions. In spite of a hindrance factor of 100 for the $E2$ probabilities, the transitions would still be expected to be predominantly electric quadrupole. (The finite probabilities for quadrupole transitions indicates that the $K$ value of one of the states involved, probably the 1.17-Mev level, is not pure.)

The assignment $I=4$ can be ruled out on the basis of the log$ft$ value of the beta transition to this state.

One would favor the assignment of positive parity to the 1.17-Mev level, as well as to all the higher excited states, on the basis of the log$ft$ values for the beta decay. However, some of these branches might be allowed transitions which are hindered by violations of selection rules for the asymptotic quantum numbers or $K$.

*States at 1.46, 1.54, and 1.64 Mev*

It is concluded that the 1.46-Mev state has spin 2 because it decays to all three members of the ground-state band. The value $I=2$ requires that $K=0$, 1, or 2. A definite choice between these possibilities is made on the basis of the relative reduced transition probabilities to the ground-state band. For quadrupole transitions, the experimental ratios are

$$B(2, I\to 4):B(2, I\to 2):B(2, I\to 0)$$
$$=(6.5\pm2):10:(0.8\pm0.3).$$

This result is clearly inconsistent with an assignment of $K=0$ or 1, but is in good agreement with the choice $K=2$ (see Table VI).

An interpretation of the 1.53-Mev state as a member of a rotational band based on the 1.46-Mev level is consistent with all of the experimental data. The energies of the levels of such a band are given by $E(I)=(\hbar^2/2\mathcal{J})[I(I+1)-K(K+1)]$, with $K=2$, $3\hbar^2/\mathcal{J}\approx0.08$ Mev, and $I=3$, 4, etc. For $I=3$, the calculated energy of the first excited state of the band is $E\approx1.54$ Mev, which agrees with the measured value well within experimental uncertainty. If the transitions to the $K=0$ band are assumed to have quadrupole character, the experimental ratios of the reduced transition probabilities are $(2.2\pm0.4):5:(\approx0)$. This is in good agreement with the theoretical ratios of 2:5:0.

The next rotational state in the $K=2$ band based on the 1.46-Mev level would be at approximately 1.64 Mev and have $I=4$. Since a state with this energy is, in fact, found in the decay scheme, the transition probabilities are again compared with the theoretical ratios of 3:1:0 in order to see if this might be the $I=4$ state. The corresponding experimental ratios are $(0.7\pm0.5):1:0$. From this disagreement, it is concluded that this state is probably not the spin-4 member of the $K=2$ rotational band. The data are not accurate enough to warrant the consideration of any other interpretation, so no conclusion is reached as to the nature of this state.

*States at 1.60 and 1.73 Mev*

The state at 1.60 Mev is observed to decay to the $0^+$ and $2^+$ members of the ground-state band. An upper limit on the intensity of a possible unobserved 1.34-Mev transition to the $4^+$ level is placed at 10% of that of the 1.60-Mev transition. A spin of either 1 or 2 would be acceptable for the 1.60-Mev state. The experimental reduced transition probabilities are

$$B(L, I\to 4):B(L, I\to 2):B(L, I\to 0)$$
$$=(<0.2):(1.4\pm0.4):1 \quad \text{for} \quad L=1,$$
$$=(<0.3):(1.5\pm0.4):1 \quad \text{for} \quad L=2.$$

From the theoretical predictions in Table VI, the values for both $I=K=2$ and $I=1$, $K=0$ lie within the experimental errors. If this level has $I=K=2$, the first excited state of a rotational band based on this level should occur at about 1.68 Mev. The failure to observe transitions to or from such a level suggests that the level at 1.60 Mev has $I=1$, $K=0$.

Several examples of states with $I=1$, $K=0$, and negative parity have been reported in even-even deformed nuclei. These are interpreted as states produced by octupole vibrations of the nuclear surface. In rotational bands accompanying these states, one finds the spin sequence 1, 3, 5, etc. If the moment of inertia of the ground-state band is used in calculating the level energies, the $I=3$ state should lie approximately 0.13 Mev above the $I=1$ state. This prediction agrees with the experimental energy for the 1.73-Mev level. For the 1.73-Mev state, only the transition to the $4^+$ level has been observed. From an estimate of the upper

limit for the intensity of the transition to the $2^+$ ($K=0$) state, the limit on the ratio of the reduced transition probabilities is calculated to be:

| Experimental | Theoretical ($I=3, K=0$) |
|---|---|
| $B(1, I\rightarrow 4)/B(1, I\rightarrow 2)=4/(\leq 3.3)$ | 4/3 |

Although this argument is not conclusive, the result is not inconsistent with this interpretation.

The interpretation of these two states as the result of an octupole vibration requires that they have negative parity. The fact that $\Delta K=2$ suggests that these allowed transitions may be expected to be hindered by a factor of the order of 100. The experimental log$ft$ values of about 6.2 and 7.6 are consistent with this interpretation.

It is of interest that in $_{68}Er^{166}$ there is a level at 1.66 Mev which has been interpreted as an octupole vibrational state with $I=1$, $K=0$, and negative parity. Since the energy of this vibrational state is not expected to vary rapidly with neutron and proton number, this information adds support to the proposed interpretation of the 1.60-Mev level in $Yb^{172}$.

## SUMMARY

From the experimental results of this study, it has been concluded that the ground-state spin of $Tm^{172}$ is $I=2$. The Nilsson level diagrams and the measured spins of neighboring nuclei combine to indicate that this state arises from the coupling of a $\frac{1}{2}^+[411]$ proton and a $\frac{5}{2}^-[512]$ neutron. This state has $K=2$ and negative parity.

The experimental data agree with the previous suggestion of a $K=0$ rotational band based on the ground state of $Yb^{172}$. The observed levels of this band are at 0.00, 0.079, and 0.260 Mev with spins and parities $0^+$, $2^+$, and $4^+$, respectively.

It is concluded that a state with $I=K=2$ exists at 1.46 Mev. This may be either an intrinsic state or a gamma vibrational state. This level is the basis of another rotational band with an excited state at 1.54 Mev ($I=3$). The second excited state of this band would be at about 1.46 Mev. A state of this energy is, in fact, observed but the experimental data are not in agreement with such an interpretation.

The properties of the state at 1.60 Mev are consistent with an assignment $I=1$, $K=0$, and it is interpreted as an octupole vibrational state. The state at 1.73 Mev can then be interpreted as a rotational state with $I=3$, $K=0$. The observed probabilities of the beta transitions to these states necessitate a breakdown of the $K$ selection rule.

The experimental data suggest the assignment $I=K=3$ for the 1.17-Mev level. A state with this spin could arise from a particle excitation.[15]

[15] For a more detailed discussion, see Argonne National Laboratory Report, ANL-6270, January, 1961 (unpublished).

## APPENDIX I. CHEMICAL SEPARATION OF RARE-EARTH ELEMENTS BY USE OF AN ION-EXCHANGE COLUMN

The basic techniques are similar to those discussed by Ketelle,[16] except that the eluting is alpha-hydroxyisobutyric acid.[17] A schematic diagram of the experimental arrangement is shown in Fig. 8. The cation-exchange resin is Berolite 220 (8% cross-linked) with a settling rate in water of $\geq 0.5$ cm/min. Circulating hot water is used to maintain the temperature of the column at approximately 80°C. Elevation of the temperature reduces the time necessary to make a separation. A column 4 mm in diameter and 7 cm long is satisfactory for separating up to about 1 mg of material. For larger amounts, a proportionately larger column is needed unless broadening of the activity peaks as a result of overloading can be tolerated. A thin glass-wool plug is placed at the top of the resin to prevent splattering of the resin when liquids are added. The flow rate of the liquid through this column is usually regulated to about 0.1 ml/min, either by adjusting the head of liquid or by applying pressure with nitrogen gas.

Before the separation, the resin is washed with 1$M$ HCl to remove complexing cations. It is then washed with several column volumes each of $H_2O$, 4$M$ $NH_4Cl$, $H_2O$, the eluting agent to be used, and finally with $H_2O$. This procedure gets the resin into the "ammoniated form" needed for the separation.

The rare-earth material is irradiated in the oxide form. After the activation, it is dissolved in 1$M$ HCl to produce the chloride. After drying to dispose of the excess HCl, the sample is picked up in a minimum amount of 0.05$M$ HCl and placed on the column. The column is allowed to drip until the active solution is lowered into the resin bed. The glass above the resin is washed with 0.05$M$ HCl, $H_2O$, and then with a few drops of the eluting agent in order to remove any active material that is not adsorbed on the resin. In each case the solution is removed by pipette down to

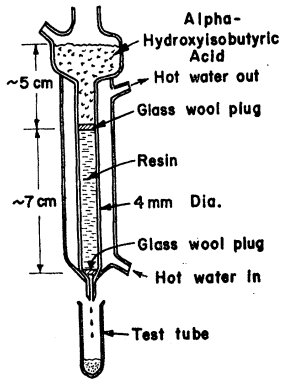


FIG. 8. Schematic diagram of ion-exchange column.

[16] B. H. Ketelle and G. E. Boyd, J. Am. Chem. Soc. **69**, 2800 (1947).

[17] G. R. Choppin and R. J. Silva, J. Inorg. & Nuclear Chem. **3**, 153 (1956); H. L. Smith and D. C. Hoffman, *ibid.* **3**, 243 (1956).

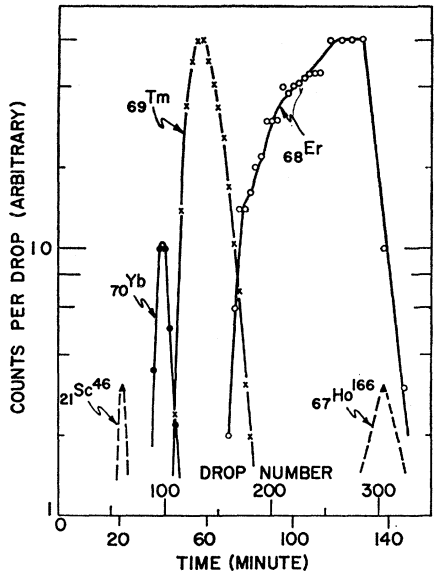


FIG. 9. Results of a separation of an erbium sample in the ion-exchange column.

the level of the glass-wool plug. The separation is started by adding alpha-hydroxyisobutyric acid.[18]

For the separation of erbium and thulium, the alpha-hydroxyisobutyric acid solution used has approximately a 0.1$M$ butyrate ion concentration and a 0.2$M$ total acid concentration.[19] This solution is made by mixing equal volumes of 0.2$M$ alpha-hydroxyisobutyric acid and 0.2$M$ ammonium alpha-hydroxyisobutyrate. The neutral salt solution is made by neutralizing a solution of the acid with ammonium hydroxide or ammonia gas to $p$H 6.4, and adjusting the final volume to give 0.2$M$ concentration. Since the ionization of the free acid is negligible and that of the ammonium salt nearly complete, the "butyrate" ion concentration (which determines the elution volume for a given element) is equal to the concentration of the ammonium salt. The acid concentration is not critical provided the final $p$H is less than 5. The $p$H of a 50–50 mixture is about 3.75. With this eluting agent the thulium and erbium are expected to be eluted from the column in about 10 and 15 free column volumes, respectively.

An example of a separation made with this procedure is shown in Fig. 9. The load consisted of 2 mg of erbium. Five drops (about 0.2 ml and about 0.33 free column volumes) were collected in each test tube. The gamma-ray spectrum of each sample was measured on the multichannel analyzer. The counting rate of a selected gamma ray related to a particular radionuclide is plotted as a function of the drop number. In general, the peaks are narrower than these. However, this curve is shown to demonstrate the relative positions of all of the elements observed in the sources.

Sources were prepared by two different methods. In the first, the active fraction from the column separation was dried a drop at a time on a backing of aluminum foil. (Heating to approximately 240°C is sufficient to volatilize the organic material.) The second method was used to prepare the source for the beta-ray spectrometer. The alpha-hydroxyisobutyric acid that contained the thulium activity was made 0.1$N$ with HCl. This solution was placed on a column of Dowex-50 resin, 2 mm in diameter and 2 cm long, and forced through with nitrogen gas. The active material that remained at the top of the column was washed successively with a few column volumes of 0.5$N$, 1$N$, and 2$N$ HCl. This process removed some unidentified impurity which had been introduced in the original separation. The thulium was then washed through the column with 6$N$ HCl and the resulting solution boiled to dryness. The thulium chloride was dissolved with water, again taken to dryness, and then dissolved in alcohol. The solution was then dried on an aluminum foil backing (1.4 mg/cm$^2$).

## APPENDIX II. COMPUTER PROGRAM FOR ANALYSIS OF BETA-RAY SPECTRA

A computer program for the analysis of experimental beta-ray spectra has been compiled for use on an IBM-704 computer by use of Fortran. The complete program consists of four independent but compatible stages. The first three stages perform the mathematical calculations associated with a "conventional" spectral analysis. The fourth stage of the program is designed to make a least-squares fit to several components simultaneously. Since the calculations of the first three stages were not readily applicable to the experimental data, only stage IV was used, and this discussion will include only those features of the computer program that are pertinent to the analysis of the beta-ray spectrum of $Tm^{172}$. A more complete report will be made at a later time.

Stage IV of the program is designed to make a least-squares fit to all or any portion of a spectrum. The shape of each component is assumed to result from a linear combination of the allowed and unique-first-forbidden spectral distributions. The complete spectrum, or any portion of it, can then be fitted to $J$ components with the function

$$\bar{N}=\sum_{j=1}^{J} m_j^2 f(\epsilon_{0j}-\epsilon)^2\{(1-\alpha_j)+\alpha_j[L_0(\epsilon_{0j}-\epsilon)^2+9L_1]\}, \quad (2)$$

for all the experimental points for which $\epsilon \leqslant \epsilon_{0j}$. If $\epsilon > \epsilon_{0j}$, the contribution from the $j$th component is

[18] The reagent used was purified by vacuum distillation through the courtesy of D. C. Stewart, Chemistry Division, Argonne National Laboratory.

[19] This mixing procedure was suggested by J. Milsted of the Atomic Energy Research Establishment, Harwell, England, at present with the Chemistry Division of Argonne National Laboratory.

zero. (Here, $m_j$ is the slope of the linearized Fermi plot of the $j$th component, $\epsilon_0$ is the end-point energy, and $\alpha$ represents the relative portion of the component which has a unique-first-forbidden spectral distribution. Also $\bar{N}_i$ is the calculated counting rate at the $i$th point, $N_i$ is the experimental counting rate, and $\sigma_i$ is the standard deviation associated with $N_i$.) The parameters to be varied in making the fit are the $m_j^2$, $\epsilon_{0j}$, and $\alpha_j$. The parameters are not allowed to vary outside of specified ranges $0 \leqslant m_j^2 \leqslant m_{\max}^2$, $1 \leqslant \epsilon_{0j} \leqslant \epsilon_{\max}$, and $0 \leqslant \alpha_j \leqslant 1$. For a particular fit, the experimental data in any region of the spectrum can be used, while the remaining part is neglected. Initial estimates must be provided for all of the $3J$ parameters. Each parameter may be either fixed at the initial estimate or permitted to vary. Also the difference in energy between the end points of any two components can be fixed.

The unfixed parameters are then varied simultaneously to obtain the minimum value of the function $\chi^2=\sum_i [(\bar{N}_i-N_i)/\sigma_i]^2$. When all the parameters cease to vary beyond some specified range, the calculation is said to have converged.

This method of analysis has several advantages over the conventional method. First, a fit can be made to a component that consists of a linear combination of the allowed and unique-first-forbidden shapes. The next advantage is that the difference in energies between any two end points, in those cases in which it is known accurately from other data, can be used. Third, when there are not enough data to permit the resolution of components differing little in energy, they can be fitted simultaneously. These three advantages are all demonstrated in the analysis of the thulium spectrum.

From the value of $\chi^2$ and the number of degrees of freedom (i.e., the number of experimental points minus the number of independent parameters), one can compute the probability $p$ of obtaining a better fit. That is, if the true spectrum is described by a function of the form (2) with the values of the parameters derived from the calculation, then $p$ is the probability that any one set of experimental data from a large group of such sets would result in a better fit (i.e., lower $\chi^2$). A value of $p$ near 1.0, for instance, may indicate that the particular form of (2) used is not correct (e.g., the number of components assumed to be present may be incorrect).

The program is also used to calculate the standard deviations associated with the best value of each of the variable parameters.